Electronic Supplementary Information for:

Fast magnetic relaxation in an octahedral dysprosium aluminate

Sonja N. König,[a] Nicholas F. Chilton,[b] Cäcilia Maichle-Mössmer,[a] Eufemio Moreno Pineda,[b] Thomas Pugh,[b] Reiner Anwander*[a] and Richard A. Layfield*[b]

[a] *Institut für Anorganische Chemie, Universität Tübingen, Auf der Morgenstelle 18, D-72076 Tübingen, Germany. E-mail: Reiner.Anwander@uni-tuebingen.de*

[b] *School of Chemistry, The University of Manchester, Oxford Road, Manchester, U.K. E-mail: Richard.Layfield@manchester.ac.uk*

General Considerations

All reactions were carried out under an inert argon or nitrogen atmosphere using standard Schlenk or glovebox (MBraun Labstar MB10, O_2 and H_2O < 0.5 ppm and MBraun MB200B, O_2 and H_2O < 0.1 ppm) techniques. The solvents were dried over Grubbs columns (MBraun, Solvent Purification System) and stored inside the glovebox or distilled over NaK (*n*-hexane) or K (thf) and stored in ampoules. Elemental Analyses were carried out on an Elementar Vario MICRO instrument. DRIFT spectra were measured on a Thermo Scientific Nicolet6700 FTIR spectrometer using KBr powder and a DRIFT cell equipped with KBr windows. The spectra were recorded with 256 scans from 4000 to 400 cm^{-1} with a resolution of 2 cm^{-1}. Dysprosium(III) chloride (99.9%) was purchased from Strem. Yttrium(III) chloride (99.9) and $AlMe_3$ (98%) were purchased from ABCR. Sodium amide (95%), *n*-butyllithum (2.5M in hexane), and $AlMe_3$ (2M in heptane) were obtained from Sigma-Aldrich. *N*-butyllithum (1.6M in hexane) was obtained from Acros as well. $LiNMe_2$ was synthesized via a modified literature procedure.[1]

Synthesis of dysprosium(III) tetramethylaluminate (1). $DyCl_3$ (2.024 g, 7.53 mmol) was suspended in thf and $LiNMe_2$ (1.153 g, 22.59 mmol) in thf was added. The slightly yellow suspension was stirred for 17 h at ambient temperature. The mixture was dried and resuspended in *n*-hexane. Then $AlMe_3$ (4.3427 g, 60.24 mmol) was added and the suspension was stirred for another 16 h, before the *n*-hexane solution was separated from the insoluble part by centrifugation. Recrystallization yielded pale yellow needles. Yield: 1.761 g, 55%
Anal. calcd. for $C_{12}H_{36}Al_3Dy$: C 34.00, H 8.56. Found: C 33.70, H 8.03. DRIFT (KBr, cm^{-1}): 2924 (m), 2886 (m), 2785 (w), 2426 (vw), 2353 (vw), 1801 (vw), 1761 (vw), 1674 (vw), 1436 (w), 1216 (m), 1193 (s), 720 (s), 698 (s), 612 (w), 569 (m), 553 (m), 465 (w), 453 (w).

Synthesis of [Dy(AlMe$_4$)$_3$] (1) doped into [Y(AlMe$_4$)$_3$]. [$Y(AlMe_4)_3$] (329 mg, 0.94 mmol) and [$Dy(AlMe_4)_3$] (20 mg, 0.05 mmol) were dissolved in 5 mL *n*-hexane and recrystallized at -30 °C. Yield: 125 mg (36%).

Crystallographic data collection and refinement

Crystals of **1** were grown by standard techniques from a saturated solution using hexane at -40 °C . Single crystals suitable for X-ray structure analyses were selected in a glovebox and coated with Paratone-N (Hampton Research). X-ray data for compound **1** was collected on a Bruker APEX II DUO diffractometer equipped with a graphite multilayer monochromator and Mo K_α radiation (λ = 0.71073 Å). Raw data were collected by using the program COSMO[2] integrated and reduced with the program SAINT[3]. Corrections for adsorption effects were applied with SHELXTL[4] and SADABS[5]. The structures were solved by direct methods and refined with standard difference Fourier techniques. CCDC 954825 contains the supplementary crystallographic data for this paper. These data can be obtained free of charge from The Cambridge Crystallographic Data Centre via www.ccdc.cam.ac.uk/data_request/cif.

Table S1. Crystal data and structure refinement for $[Dy(AlMe_4)_3]$ (**1**).

CCDC	954825
Empirical formula	$C_{12}H_{36}Al_3Dy$
Formula weight	423.85
T/K	100
λ/Å	0.71073
Crystal system	Monoclinic
Space group	$P2_1/c$
a/Å	7.3556(10)
b/Å	17.681(2)
c/Å	32.162(4)
α/°	90
β/°	92.518(4)
γ/°	90
V/Å^3	4178.7(9)
Z	8
Density (calcd.)/Mg m^{-3}	1.347
Crystal size/mm^3	0.34 × 0.29 × 0.18
Theta range /°	1.3 to 28.3
Reflections collected	40025
Independent reflections	10367 [R(int) = 0.030]
Completeness/%	99.6
Data/restraints/parameters	10367/0/313
Goodness-of-fit on F^2	1.082
Final R indices [$I>2\sigma(I)$]	R_1 = 0.0258, wR_2 = 0.0554
R indices (all data)	R_1 = 0.0292, wR_2 = 0.0566
Largest diff. peak and hole/e.Å^{-3}	0.602 and -0.730

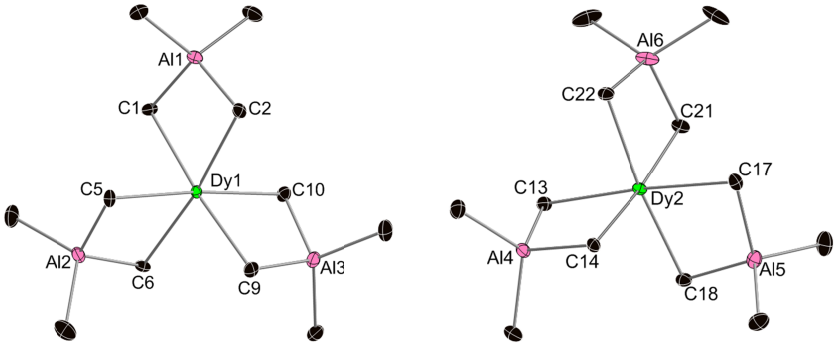

Figure S1. Molecular structure of 1a (left) and **1b** (right) with thermal ellipsoids at 50%. Hydrogen atoms not shown.

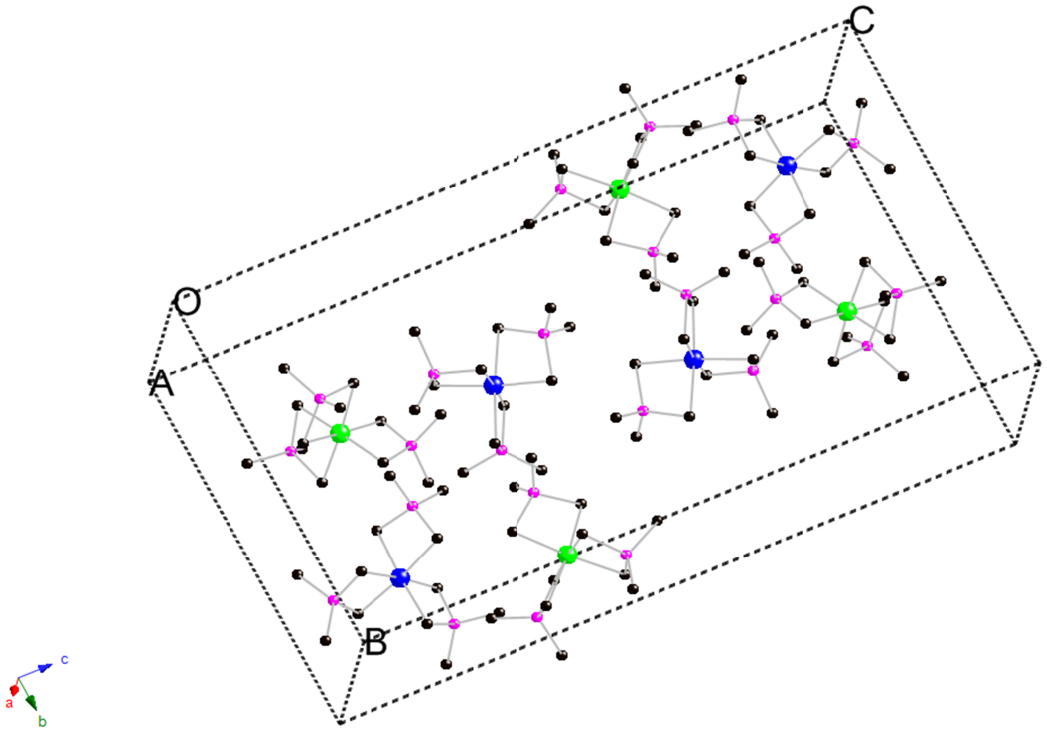

Figure S2. Unit cell of **1**. Complex **1a** has green Dy atoms and complex **1b** has blue Dy atoms.

Table S2. Selected bond lengths and angles for complexes **1a** and **1b**.

1a		**1b**	
Dy(1)–C(1)	2.540(3)	Dy(2)–C(13)	2.514(3)
Dy(1)–C(2)	2.512(3)	Dy(2)–C(14)	2.517(3)
Dy(1)–C(5)	2.523(3)	Dy(2)–C(17)	2.523(3)
Dy(1)–C(6)	2.523(3)	Dy(2)–C(18)	2.526(3)
Dy(1)–C(9)	2.540(3)	Dy(2)–C(21)	2.535(3)
Dy(1)–C(10)	2.514(3)	Dy(2)–C(22)	2.531(3)
C(1)-Dy(1)-C(2)	84.28(9)	C(13)-Dy(2)-C(14)	84.8(1)
C(1)-Dy(1)-C(5)	91.2(1)	C(13)-Dy(2)-C(18)	92.6(1)
C(1)-Dy(1)-C(6)	90.40(9)	C(13)-Dy(2)-C(21)	93.3(1)
C(1)-Dy(1)-C(10)	92.4(1)	C(13)-Dy(2)-C(22)	91.93(1)
C(2)-Dy(1)-C(5)	91.2(1)	C(14)-Dy(2)-C(17)	91.32(9)
C(2)-Dy(1)-C(9)	92.4(1)	C(14)-Dy(2)-C(18)	93.2(1)
C(2)-Dy(1)-C(10)	92.2(1)	C(14)-Dy(2)-C(22)	90.8(1)
C(5)-Dy(1)-C(6)	84.75(9)	C(17)-Dy(2)-C(18)	85.0(1)
C(5)-Dy(1)-C(9)	92.0(1)	C(17)-Dy(2)-C(21)	90.8(1)
C(6)-Dy(1)-C(9)	93.1(1)	C(17)-Dy(2)-C(22)	90.8(1)
C(6)-Dy(1)-C(10)	92.3(1)	C(18)-Dy(2)-C(21)	91.5(1)
C(9)-Dy(1)-C(10)	84.65(9)	C(21)-Dy(2)-C(22)	84.6(1)
C(1)-Dy(1)-C(9)	175.5(1)	C(13)-Dy(2)-C(17)	175.3(1)
C(2)-Dy(1)-C(6)	173.2(1)	C(14)-Dy(2)-C(21)	175.0(1)
C(5)-Dy(1)-C(10)	175.4(1)	C(18)-Dy(2)-C(22)	174.22(9)

1. H. Gilman and H. W. Melvin, Jr., *J. Am. Chem. Soc*., 1950, **72**, 995.
2. *APEX v. 2008.5-0*, Bruker ASX, Madison, 2008
3. *Bruker Saint v. 756A*, Bruker AXS, Madison, 2009
4. Sheldrick, G. M. *Acta Crystallogr., Sect. A: Found. Crystallogr.,* 2008, **64**, 112
5. Sheldrick, G. M. *SADABS v. 2008/1*, University of Göttingen, Göttingen, 2008

Computational details

Calculations were performed using the X-ray crystal geometry with no optimization. Both unique dysprosium sites in the asymmetric unit were evaluated, Dy(1) and Dy(2), which correspond to the crystallographic labelling. The *ab-initio* calculations were performed using the CASSCF/ CASSI approach in MOLCAS 7.8.[6-8] The Complete Active Space methodology was used to accurately model the orbital degeneracy of the 4f orbitals of dysprosium(III), where the active space was 9 electrons in 7 orbitals, CAS(9,7). The ANO-RCC basis sets were used exclusively, where dysprosium was treated with VQZP quality, the six carbon atoms in closest proximity to the dysprosium were treated with VTZP quality and all other atoms were treated with VDZP quality. The calculations employed the second order Douglas-Kroll-Hess Hamiltonian, where scalar relativistic contractions are taken into account in the basis set and the spin-orbit coupling is handled separately in the CASSI procedure. The *g*-tensors for the Kramers doublets of Dy^{III} were calculated based on the pseudo-spin $\tilde{S} = \frac{1}{2}$ formalism.[9] In the CASSCF procedure, the sextets were given 21 roots, the quartets were given 224 roots and the doublets were given 158 roots. In the CASSI procedure, 21 sextets, 128 quartets and 130 doublets were mixed by spin-orbit coupling.

Table S3. Electronic properties for the eight Kramers doublets of the ground $^6H_{15/2}$ multiplet of Dy(1) in complex **1a**.

Energy (cm^{-1})	g_x	g_y	g_z	Angle (°)
0.0	0.10	3.04	15.73	-
10.9	0.18	2.99	14.77	38.7
29.4	0.06	0.16	18.57	80.5
124.8	3.37	6.56	11.08	16.5
163.5	0.78	2.34	9.24	74.0
201.2	0.92	3.48	9.97	75.4
248.7	2.28	3.08	13.85	63.5
358.8	0.05	0.08	19.16	75.6

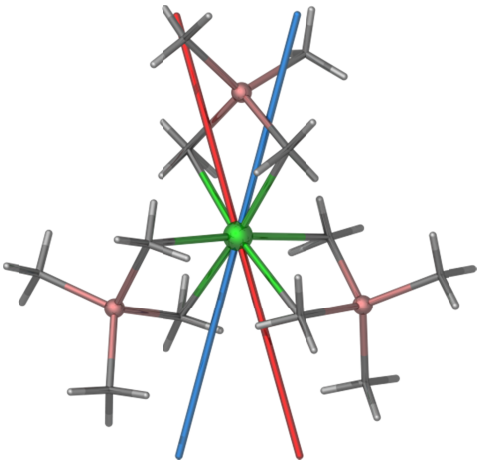

Fig. S3. Orientation of the main magnetic moments of the ground (blue rod) and first excited (red rod) Kramers doublets of Dy(1) in **1a**. Dy = green, Al = pink, C = grey, H = white.

Table S4. Electronic properties for the eight Kramers doublets of the ground $^6H_{15/2}$ multiplet of Dy(2) in complex **1b**.

Energy (cm^{-1})	g_x	g_y	g_z	Angle (°)
0.0	0.03	0.55	18.41	-
19.9	0.06	0.54	17.27	63.1
37.8	0.04	0.17	18.73	81.7
137.7	2.67	4.27	12.68	26.1
177.5	2.65	3.86	8.52	89.9
204.6	2.67	2.88	8.93	64.4
245.7	3.15	4.28	12.68	63.8
336.0	0.10	0.11	19.12	68.2

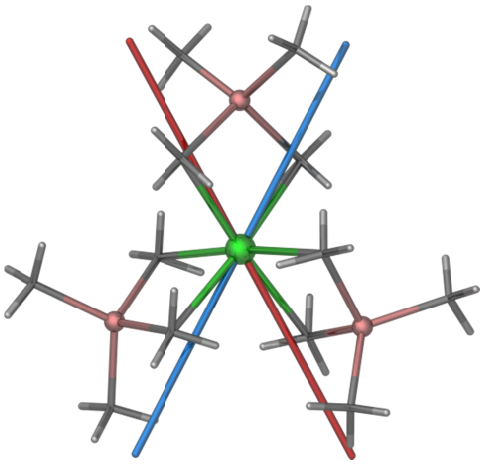

Fig. S4. Orientation of the main magnetic moments of the ground (blue rod) and first excited (red rod) Kramers doublets of Dy(2) in **1b**. Dy = green, Al = pink, C = grey, H = white.

6. G. Karlström, R. Lindh, P.-Å. Malmqvist, B. O. Roos, U. Ryde, V. Veryazov, P.-O. Widmark, M. Cossi, B. Schimmelpfennig, P. Neogrady, and L. Seijo, *Comput. Mater. Sci.*, 2003, **28**, 222–239.
7. V. Veryazov, P. Widmark, L. Serrano-Andrés, R. Lindh, and B. O. Roos, *Int. J. Quantum Chem.*, 2004, **100**, 626–635.
8. F. Aquilante, L. De Vico, N. Ferré, G. Ghigo, P. Malmqvist, P. Neogrády, T. B. Pedersen, M. Pitoňák, M. Reiher, B. O. Roos, L. Serrano-Andrés, M. Urban, V. Veryazov, and R. Lindh, *J. Comput. Chem.*, 2010, **31**, 224–247.
9. H. Bolvin, *ChemPhysChem*, 2006, **7**, 1575–1589.

Magnetic property measurements

The magnetic properties of a polycrystalline sample of **1**, and of **1** diluted into $[Y(AlMe_4)_3]$ (both unrestrained), were measured using a Quantum Design MPMS-7 SQUID magnetometer at temperatures in the range 1.8-300 K. In a glove box, the polycrystalline samples were transferred to Kel-F capsules, which were then sealed with an O-ring cap, and the capsules were then placed in plastic straws. One end of the straw was then sealed with a cap, and the other end was sealed with Blu-Tac. The straw was then sealed in a Schlenk tube and taken to the magnetometer. The straw was removed from the Schlenk tube and the Blu-Tac quickly replaced with the carbon fibre rod, and then the sample was quickly transferred to the purged sample space of the MPMS. All ac susceptibility measurements used an oscillating field of H_{ac} = 1.55 Oe.

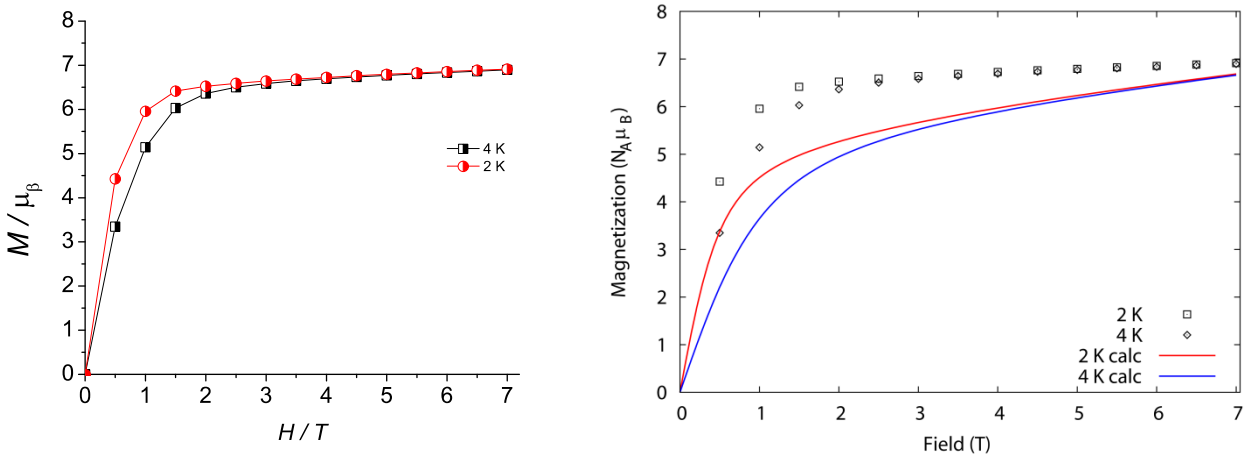

Fig. S5. Left: plot of experimental magnetization vs. field at various temperatures for undiluted **1**, in which the solid lines are a guide for the eye. Right: comparison of the experimental (points) and ab-initio calculated (solid lines) magnetization. The experimental magnetization increases more rapidly that the calculated magnetization, however the 7 T saturation values are very similar.

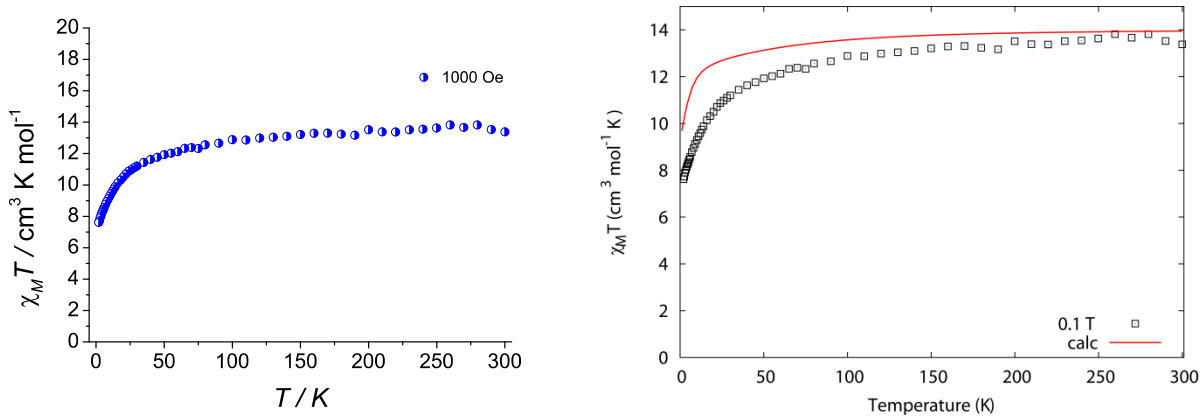

Fig. S6. Left: plot of experimental $\chi_M T$ vs. T for undiluted **1** in an applied field of H_{dc} = 1000 Oe. Right: comparison of the experimental (points) and ab-initio calculated (solid lines) susceptibility.

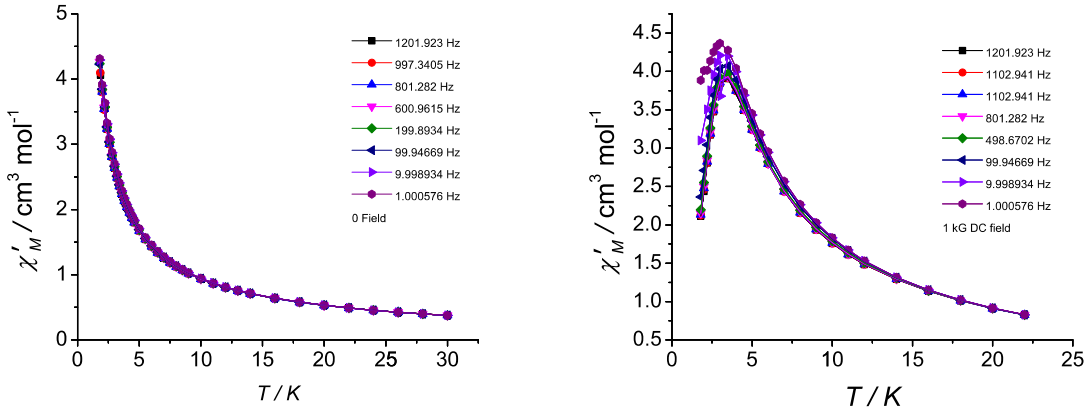

Fig. S7. χ' vs. temperature at various ac frequencies for undiluted **1**. Left: $H_{dc} = 0$. Right: $H_{dc} = 1000$ Oe. The solid lines connecting the data points are a guide for the eye.

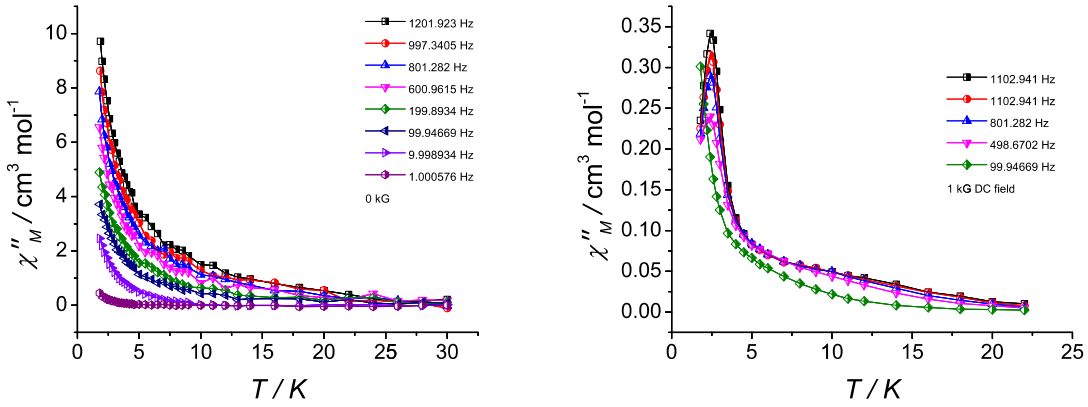

Fig. S8. χ'' vs. temperature at various ac frequencies for undiluted **1**. Left: $H_{dc} = 0$. Right: $H_{dc} = 1000$ Oe. The solid lines connecting the data points are a guide for the eye.

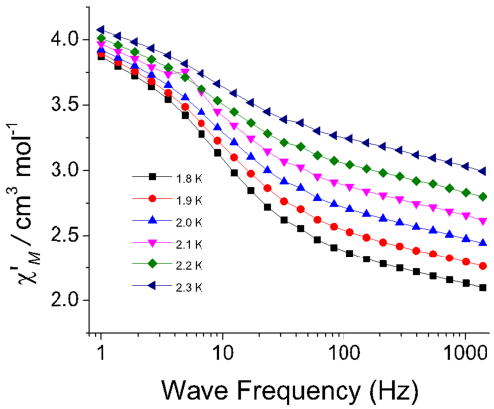

Fig. S9. χ'' vs. ac frequency at various temperatures for undiluted **1**, with $H_{dc} = 1000$ Oe. The solid lines connecting the data points are a guide for the eye.

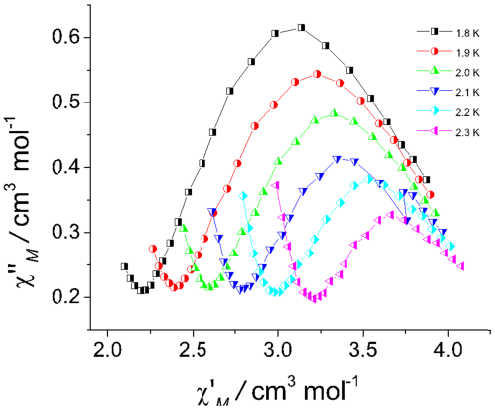

Fig. S10. Cole-Cole plot of χ'' vs. χ' for undiluted **1** in an applied field of H_{dc} = 1000 Oe. The solid lines connecting the data points are a guide for the eye.

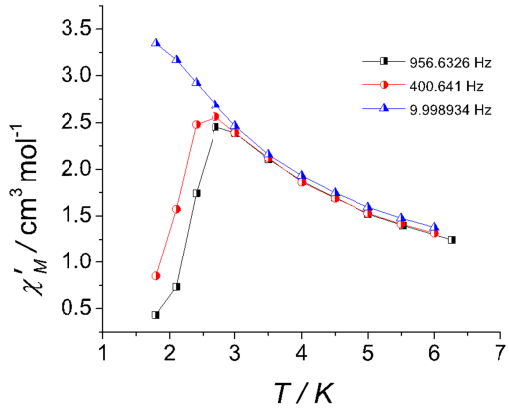

Fig. S11. χ' vs. temperature at various ac frequencies for diluted **1**, with H_{dc} = 1000 Oe. The solid lines connecting the data points are a guide for the eye.

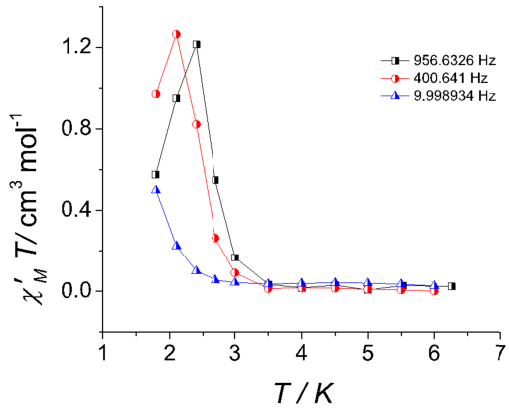

Fig. S12. χ'' vs. temperature at various ac frequencies for diluted **1**, with H_{dc} = 1000 Oe. The solid lines connecting the data points are a guide for the eye.

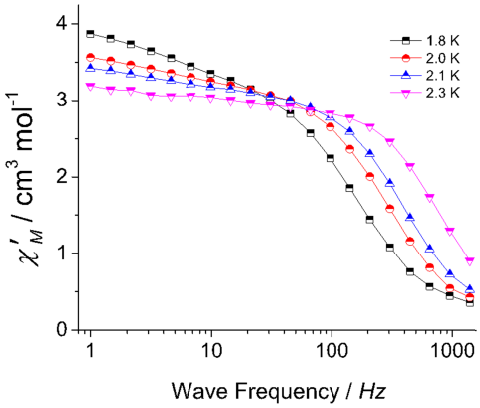

Fig. S13. χ' vs. ac frequency at various temperatures for diluted **1**, with H_{dc} = 1000 Oe. The solid lines connecting the data points are a guide for the eye.

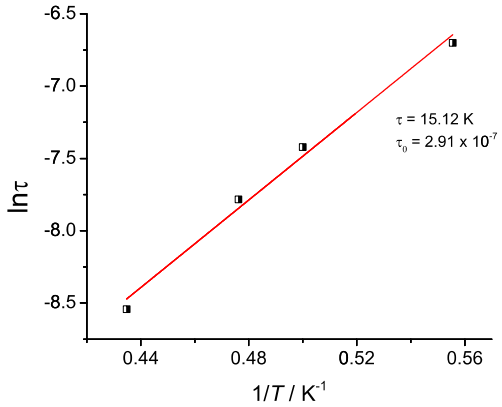

Fig. S14. Arrhenius plot of ln (τ/s) vs. (1/T) for magnetically dilute 1 in an applied of H_{dc} = 1000 Oe.

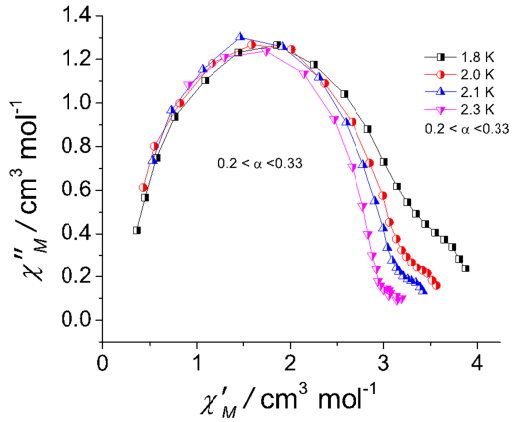

Fig. S15. Cole-Cole plot of χ'' vs. χ' for diluted **1** in an applied field of H_{dc} = 1000 Oe. The solid lines connecting the data points are a guide for the eye.